

Numerical Simulations and Kinetic Theory of Bubbly Liquids Rheology Under Microgravity

Sang-Yoon Kang[†] and Ashok A. Sangani*

Department of Chemical Engineering, Korea Advanced Institute of Science and Technology, Daejeon 305-701, Korea

*Department of Chemical Engineering and Material Science, Syracuse University, Syracuse, NY 13244, U.S.A.

(Received 31 October 2001 • accepted 14 February 2002)

Abstract—Simple shear flows of dilute suspensions of spherical bubbles at large Reynolds numbers are studied by using numerical simulations and kinetic theory. It is shown that the mean-square bubble velocity is very sensitive to the volume fraction and Reynolds number of the bubbles as well as on initial conditions. The balance of energy contained in bubble velocity fluctuations plays an important role in the rheology of the dispersed phase, which is generally non-Newtonian.

Key words: Bubbly Liquids, Simulation, Soft Core Potential, Runge-Kutta Algorithm, Kinetic Theory

INTRODUCTION

Bubbles suspended in a liquid are found in nature and in many industrial processes such as bubble columns [Bando et al., 2000; Kim et al., 2002] and centrifuges in the petrochemical industry, cooling devices of nuclear-reactor systems and air entrained in the form of bubbles in rivers and at the surface of the oceans. Therefore, it is desirable to develop an analytical framework for predicting macroscopic behavior of bubble suspensions. A series of recent papers [Biesheuvel and Gorissen, 1990; Sangani and Didwania, 1993a; Zhang and Prosperetti, 1994; Bulthuis et al., 1994] provide a rigorous derivation of the equations of motion for a suspension of bubbles with potential flow interactions. An important property arising in these equations is the dispersed-phase pressure tensor, which depends on hydrodynamic and collisional interactions between the bubbles and also on their velocity distribution.

A uniform suspension of bubbles rising due to their buoyancy is subject to instabilities that lead to volume fraction variations. One mechanism that has long been studied is the instability to void fraction waves resulting from the bubble's added mass and the dependence of the drag force on volume fraction [Biesheuvel, 1995]. Sangani and Didwania [1993b] and Smereka [1993] have recently observed a second instability mechanism in dynamic simulations of potential flow. Their simulations showed that bubbles form large clusters in planes normal to gravity. In other words, the uniform state of bubble suspension in the presence of nonzero mean relative motion between the bubbles and surrounding liquid is generally unstable. The basic mechanism by which this instability occurs is as follows. According to the potential flow theory, the pressure in the fluid between two bubbles rising side by side is lower than the pressure away from the bubbles. This Bernoulli effect causes an attractive force between pairs of bubbles that are oriented horizontally. Similar consideration of two bubbles oriented vertically and rising through a liquid shows that there will be a repulsive force between them causing them to move away from each other. Thus,

in a suspension containing many bubbles, pairs of bubbles aligned horizontally occur quickly and grow further with time to form clusters in horizontal planes. The observed instability in the numerical simulations was thus explained in terms of microscale forces occurring between pairs of bubbles. In either case, the mechanism that may tend to stabilize the homogeneous suspension is the positive bubble pressure created by fluctuations in the bubble velocities.

The purpose of the present work is to determine the distribution of bubble velocities in a suspension of bubbles subject to simple shear flow with potential flow interactions among the bubbles. This will be accomplished by using a numerical simulation method similar to that developed in Sangani and Didwania [1993b] and the results of the simulation will be interpreted by using kinetic theories. It will be seen that the bubble collisions induced by shearing motion can provide a quite effective mechanism for enhancing the bubble velocity fluctuations.

The application of results based on the potential flow interactions to physical systems must be approached with caution. The potential flow approximation is rigorously valid for bubbles with slip boundary conditions in the dual limits of high Reynolds number and low Weber number (so that bubble deformation can be neglected).

The best system for approaching these limits is bubbles with diameters of about 1 mm in water for which the Reynolds number is about 130 and the Weber number about 0.5. Even in this case the limits are only approximately satisfied and the value of the potential flow approximation may depend upon the nature of the interactions being described. For example, potential flow would be expected to be more accurate for collision between bubbles moving with substantially different speeds in different directions than when the bubbles rise at nearly the same velocity. In more general circumstances, such as solid-liquid or liquid-liquid suspensions and suspensions of bubbles with larger diameters (4 mm), which are typical of most of the experimental literature, boundary layer separation plays an important role in the dynamics.

Other methods currently under development [Ladd, 1990] show promise for the possibility of simulating suspensions including bubble deformation and continuous phase vorticity. However, we believe that the relatively extensive simulation results and the mecha-

[†]To whom correspondence should be addressed.

E-mail: kangsa@mail.kaist.ac.kr

nistic understanding that can be developed for bubbles with potential flow interactions will provide a useful reference for understanding these more complex suspensions.

In section 2 we briefly describe the numerical simulation procedure and in section 3 we present the results of simulations and an approximate kinetic theory of *dilute* bubbly liquids. We find that the steady state velocity variance depends, in a rather complicated manner, on the volume fraction ϕ of bubbles and the Reynolds number Re_s based on shear rate. At large Re_s and small ϕ , we find multiple steady states: if the initial variance is relatively large, then the final state variance is very large, of $O((Re_s/\phi)^2)$. We refer to this as an ignited state. On the other hand, if the initial variance is small, then the steady state, which we refer to as a quenched state, has a vanishingly small variance.

The multiple steady states are shown to arise due to nonlinear dependence of the dispersed-phase shear viscosity on the velocity variance of bubbles or, equivalently, the temperature of the dispersed-phase. We also find that the multiple steady states are observed only when $Re_s > 88$ and ϕ is sufficiently small ($\phi < \phi_c(Re_s)$). For smaller Re_s , the final state is quenched regardless of the initial conditions, and for $Re_s > 88$ and $\phi > \phi_c(Re_s)$, the final steady state is always ignited. We also find that the dispersed-phase rheology exhibits normal stress differences. Finally, in section 4 we assess approximate conditions under which the shear-induced variance may be significant in stabilizing flows of bubbly liquids through pipes.

The results presented here are preliminary and limited to dilute bubbly liquids. We plan to report more complete investigation including the simulations and theory for non-dilute bubbly liquids and the question of stability of bubbly liquids under simple shear and gravity in a future publication.

THE SIMULATION METHOD

The simulation method is described in detail in Sangani and Didwania [1993b]. Here, we briefly summarize the method indicating some modifications we have made in the present study. We consider motion of N spherical bubbles of radius a placed within a unit cell of periodic array. The velocity \mathbf{w}^α of a representative bubble α is written as a sum of the ensemble-averaged mixture velocity $\langle \mathbf{u} \rangle$ and a relative velocity \mathbf{V} :

$$\mathbf{w}^\alpha(t) = \langle \mathbf{u} \rangle(\mathbf{x}^\alpha, t) + \mathbf{V}^\alpha(t), \quad (1)$$

where \mathbf{x}^α is the position of the center of the bubble at time t . Similarly, the velocity of the fluid $\mathbf{u}(\mathbf{x}, t) = \langle \mathbf{u} \rangle + \mathbf{u}'$ is written as a sum of $\langle \mathbf{u} \rangle$ and \mathbf{u}' where \mathbf{u}' is the disturbance flow induced by the bubbles moving with the relative velocity $\mathbf{w}^\alpha(t)$. Disturbance \mathbf{u}' is assumed to depend only on the position and the relative velocities of the bubbles. Thus, by definition $\langle \mathbf{u}' \rangle = \mathbf{0}$. In simulations we enforce this condition by requiring that the average of \mathbf{u}' over the unit cell vanishes at any given instant. We are interested in a large Reynolds number situation where the hydrodynamic interactions are dominated by potential flow, and therefore we write $\mathbf{u}' = \nabla \varphi$ and solve $\nabla^2 \varphi = 0$, subject to the boundary condition $\nabla \varphi \cdot \mathbf{n} = \mathbf{V}^\alpha \cdot \mathbf{n}$ on the surface of bubbles. Here, \mathbf{n} is the unit outward normal vector on the surface of the bubble α . As shown in Sangani et al. [1991] and in Sangani and Didwania [1993b], the velocity potential can be determined to a very good accuracy with a point-dipole approximation

$$\varphi = \mathbf{G} \cdot \mathbf{x} - \sum_{\alpha=1}^N \mathbf{D}^\alpha \cdot \nabla S_1(\mathbf{x} - \mathbf{x}^\alpha), \quad (2)$$

where S_1 is a Green's function for Laplace equation in a periodic domain [Hasimoto, 1959; Sangani et al., 1991] and \mathbf{D}^α is the dipole strength. The condition that the average of \mathbf{u}' over the unit cell must vanish is satisfied by taking (cf. Sangani and Didwania [1993b]).

$$\mathbf{G} = (4\pi/\tau) \sum_{\alpha=1}^N \mathbf{D}^\alpha \quad (3)$$

where τ is the volume of the unit cell. Physically, \mathbf{G} is the back flow caused by the relative motion of the bubbles. To calculate the trajectory of bubbles we must apply force balance on each bubble (assumed to be massless). The impulse defined by $\mathbf{I}^\alpha = -\rho \int_{S_\alpha} \varphi \mathbf{n} ds$ plays a role analogous to the momentum of a particle in Newtonian mechanics. We write the force balance as

$$\frac{d\mathbf{I}^\alpha}{dt} = \mathbf{F}^\alpha = \mathbf{F}_g + \mathbf{F}_v + \mathbf{F}_u + \mathbf{F}_p + \mathbf{F}_c, \quad (4)$$

where $\mathbf{F}_g = -4\pi a^3/3 \mathbf{g}$ is a force due to buoyancy, \mathbf{F}_v is a viscous force, \mathbf{F}_u is a force due to temporal and spatial variations in the ensemble-averaged velocity $\langle \mathbf{u} \rangle$ of the mixture, \mathbf{F}_c is a force on the bubble during its collision with other bubbles, \mathbf{F}_p is a force due to potential flow interactions. As shown in Sangani and Didwania [1993a], the last quantity is evaluated from

$$\mathbf{F}_p = -4\pi \rho \sum_{\gamma=1}^N \mathbf{D}^\alpha \mathbf{D}^\gamma : \nabla \nabla \nabla S_1(\mathbf{x}^\alpha - \mathbf{x}^\gamma), \quad (5)$$

where the singular part of S_1 must be removed from S_1 for $\gamma = \alpha$ before evaluating the third derivative of S_1 . The viscous force is evaluated by using a method described in Sangani and Didwania [1993b]. The main modifications in the present study are concerned with the evaluation of \mathbf{F}_u and \mathbf{F}_c . In Sangani and Didwania [1993b] we considered a special case of constant average velocity, whereas in the present study we are interested in the case of simple shear. For this purpose we use a slightly modified version of the expression proposed by Auton et al. [1988]

$$\mathbf{F}_{u,i}^\alpha = m \frac{D\langle u_i \rangle}{Dt}(\mathbf{x}^\alpha) - I_i^\alpha \frac{\partial \langle u_i \rangle}{\partial x_i}(\mathbf{x}^\alpha), \quad (6)$$

where the derivatives of $\langle \mathbf{u} \rangle$ are evaluated at $\mathbf{x} = \mathbf{x}^\alpha$, $m = 4\pi \rho a^3/3$ is the mass of fluid having the same volume as the bubble and $D/Dt = \partial/\partial t + \langle \mathbf{u} \rangle \cdot \nabla$ is a time derivative following the average motion of the mixture. While we do not discuss about using (6), this relation is consistent with several known results. The above expression can be shown to give the correct force on a bubble for the cases of (i) a small amplitude oscillatory flow examined in Sangani et al. [1991], (ii) pure extensional flow $\langle u_i \rangle = e_{ij} x_j$ with $e_{ij} = e_{ji}$, at least for which the flow is irrotational, and (iii) the simple shear flow past a single spherical bubble with weak shear. No restrictions on the magnitude of ϕ are needed for the validity of (6) in the above two cases. Finally, (6) also gives the correct lift force on a bubble in dilute dispersions in the presence of simple shear, for which the magnitude of vorticity is small compared to V/a where V is a characteristic magnitude of bubbles' relative velocity. Thus, we expect it to provide a very good approximation for ignited states. Note that for the case of an isolated bubble with velocity V_j^α , the expression (6) reduces to the

one given by Auton et al. [1988] upon substituting $I^{\alpha} = mV^{\alpha}/2$.

In simulations of non-deformable bubbles with potential flow, it is commonly observed that the bubbles will come into contact while still moving at a finite relative velocity. In a physical suspension such a collision could lead to a bubble bounce or to coalescence depending on the Weber number based on the relative velocity. For the sake of simplicity in the simulation, it is convenient to assume that the bubbles always bounce and this can be achieved in practice without violating the free slip boundary condition on the bubble surface through the addition of salt to the suspending water [Lessard and Zieminski, 1971; Tsao and Koch, 1994]. Thus, we include a collisional force in the simulations to achieve an energy and momentum conserving bubble bounce. The collisional force \mathbf{F}_c^{α} was evaluated in Sangani and Didwania [1993b] by assuming the collision process to be instantaneous and momentum conserving. This has some difficulties in numerical implementation. To overcome this we used a soft core repulsive potential to model the collision process. Specifically, the collision force was taken to be

$$\mathbf{F}_c^{\alpha} = -\nabla_{\alpha} \varphi_c \quad \text{with} \quad \varphi_c = \sum_{\alpha=1}^N \sum_{\gamma=1}^N \Gamma_{\alpha\gamma} [2a - |\mathbf{x}^{\alpha} - \mathbf{x}^{\gamma}|]^3. \quad (7)$$

Here $\Gamma_{\alpha\gamma}$ if bubbles α and γ are not overlapping. Otherwise, $\Gamma_{\alpha\gamma} = \Gamma_c \Delta_{\alpha\gamma}^{\alpha\gamma}$ where Γ_c is a constant and $\Delta_{\alpha\gamma}^{\alpha\gamma}$ is the component of the relative velocity $\mathbf{V}^{\alpha} - \mathbf{V}^{\gamma}$ along the line joining the position of the bubbles at the onset of overlap.

The numerical algorithm consisted of determining the force on each bubble given position and impulse of all the bubbles in the suspension and integrating $\mathbf{I}^{\alpha} = \mathbf{F}^{\alpha}$ and $\mathbf{x}^{\alpha} = \mathbf{v}^{\alpha}$ using a fourth-order Runge-Kutta scheme. This method is more efficient and faster than the modified Euler algorithm used in Sangani and Didwania [1993b] for the integration of time. In the Runge-Kutta scheme, bubbles can be slightly overlapped depending on the time step inducing the inclusion of collisional force from soft core potential in determining new velocities of bubbles. The time step for integration was chosen to scale with the root-mean-squared velocity of the bubbles.

SIMULATION RESULTS AND KINETIC THEORY FOR SIMPLE SHEAR MOTION

In this paper we shall consider simple shear motion of dilute bub-

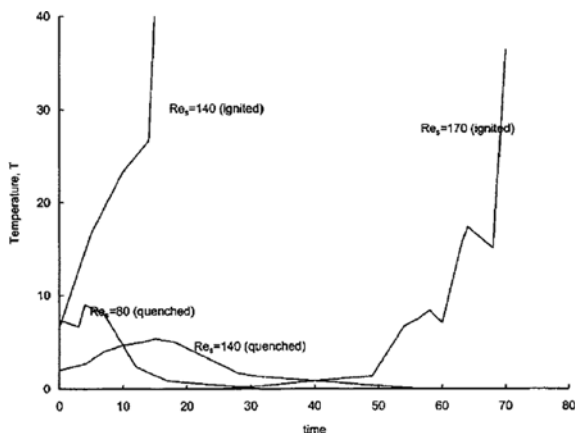


Fig. 1. Temperature as a function of time, initial condition at various Reynolds numbers and volume fraction $\phi=0.005$.

bly liquids under microgravity, i.e. $\mathbf{g}=\mathbf{0}$, and $\langle \mathbf{u} \rangle = \gamma \mathbf{x} \cdot \delta_1$. The distances are rendered non-dimensional with a , the velocity with a , and the time with $1/\gamma$. Typical simulation results are illustrated in Fig. 1 which shows velocity variance $\langle \mathbf{V}^2 \rangle$ as a function of time for $\phi=0.005$ at three different Reynolds numbers $Re_s = \gamma a^3/\mu$. We see that the final steady state, at $Re_s=140$, depends on the initial conditions of velocity variance. If the bubble suspension is stirred sufficiently before shearing, then the final state has very large velocity fluctuations. We shall refer to this as the *ignited state*. If, on the other hand, the initial velocity fluctuations are small, then the final state has very small velocity fluctuations; the bubbles essentially follow the imposed shear. We shall refer to this as the *quenched state*. Such multiple steady states are not observed for all Re_s and ϕ , the volume fraction of bubbles. For example, as seen in Fig. 1, the final state is the ignited state when $Re_s=170$ regardless of the initial conditions. And, similarly, the final state is always the quenched state when $Re_s=80$.

Before we present an approximate kinetic theory and a more detailed comparison between the theory and numerical simulations, it will help to have a qualitative understanding of the phenomenon. The steady state variance is determined by balancing between the energy input in shearing the dispersion and the viscous energy dissipation as shown in Fig. 2 graphically. The former can be approximated to equal $\mu_s^* \gamma^2$ while the latter to $12\pi\mu n a \langle \mathbf{V}^2 \rangle$. Energy input by shearing has non-linear dependence on velocity variance whereas energy loss due to viscous dissipation is linearly dependent on temperature. From this balance, two stable solutions and one unstable solution exist. The steady state is reached relying on the initial velocity variance. When the initial variance is below the unstable solution, the quenched state is reached. The ignited state will be accomplished when the initial variance is above the unstable solution. As volume fraction increases, the energy input line will shift to dotted line resulting in one stable steady state at higher volume fractions. Here, μ_s^* is the (dimensional) dispersed-phase shear viscosity, n is the number density of bubbles, and $\langle \mathbf{V}^2 \rangle$ is the dimensional velocity variance. In the ignited state, the collision time $\tau_c = a/(\phi \langle \mathbf{V}^2 \rangle^{1/2})$ is much shorter than the viscous relaxation time $\tau_v = pa^2/(18\mu)$, and the leading order velocity distribution as $Re_s \rightarrow \infty$ is isotropic Maxwellian owing to rigorous collisions of bubbles. Thus we can estimate μ_s^* from the kinetic theory of gases by taking the mass of bubbles to be their virtual mass $m/2$ and the mean free path to be a/ϕ to yield $\mu_s^* \sim pa \langle \mathbf{V}^2 \rangle^{1/2}$. The energy balance then shows

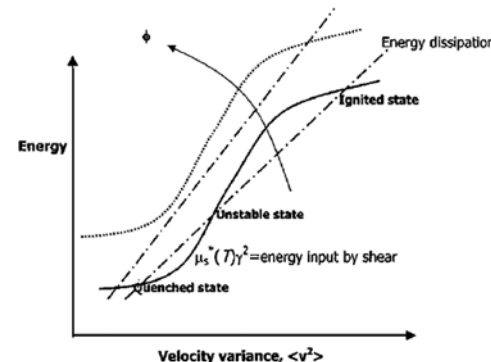


Fig. 2. Graphical demonstration of multiple steady states in sheared bubble suspension.

that $\langle \mathbf{V}^2 \rangle \sim (\text{Re}_s/\phi)^2 \gamma^2 a^2$. In the quenched state, $\langle \mathbf{V}^2 \rangle$ is very small, and, consequently, $\tau_v \ll \tau_c$. Thus, the majority of the bubbles move with the velocity of the fluid. The velocity distribution is expected to be very different from Maxwellian because bubbles relax close to the local fluid velocity. The initial conditions influence the final steady state for intermediate values of Re_s by setting up the initial value of the collision time. At smaller Re_s , the viscous relaxation time is small enough to dissipate the fluctuations leading always to the quenched state while the fluctuations induced by the imposed shear are sufficient at large enough Re_s to eventually make $\tau_c \ll \tau_v$, corresponding to the ignited state.

1. Kinetic Theory

For a spatially homogeneous dispersion of bubbles, the velocity distribution function $f(\mathbf{V})$ satisfies

$$\frac{\partial f}{\partial t} + \nabla_v \cdot (\mathbf{V} f) = 0 \quad (8)$$

Since ϕ is very small, the bubbles only undergo occasional interactions. It is well known that potential flow bubbles often undergo actual collisions and Tsao and Koch [1994] showed that for low Weber number bubbles with short-range repulsive forces these collisions are nearly elastic. In this simple kinetic theory we will neglect the hydrodynamic interactions between bubbles and treat the collisions as perfectly elastic. Substituting in (4) $\mathbf{F}_g = \mathbf{F}_p = \mathbf{0}$, $\mathbf{F}_v = -12\pi\mu a \mathbf{V}$, $\mathbf{I} = m\mathbf{V}/2$, $\mathbf{F}_{\text{coll},i} = -(1/2)m\mathbf{V}_i \delta_{i2}$ (lift force), expressing the contribution due to the collisional force in the notation of Chapman and Cowling [1970], and non-dimensionalizing we obtain

$$\frac{\partial f}{\partial t} - \frac{\partial}{\partial V_k} [(\delta_{i2} V_i + St^{-1} V_k) f] = \frac{\partial_e f}{\partial t} \quad (9)$$

where the Stokes number, $St = \text{Re}_s/18 = \gamma\tau_v = \rho\gamma a^2/(18\mu)$, is a non-dimensional viscous relaxation time and $\partial_e f/\partial t$ is the rate of change in f at a fixed point due to collisional encounters. As shown in Chapter 3 of Chapman and Cowling, this latter quantity is expressed in terms of an integral

$$\frac{\partial_e f}{\partial t} = \iint d\mathbf{w}_i d\mathbf{k}_i [f(\mathbf{w}') f(\mathbf{w}'_i) - f(\mathbf{w}) f(\mathbf{w}_i)] \quad (10)$$

Here, $\mathbf{w} = \langle \mathbf{w} \rangle + \mathbf{V}$ is the velocity of a representative bubble in collision with another bubble with velocity \mathbf{w}_i , the velocities of the bubbles at the end of the collision encounter being \mathbf{w}' and \mathbf{w}'_i , and \mathbf{k} and \mathbf{k}_i are parameters that depend on the relative velocities and orientation of the bubbles at the onset of the collision. For small ϕ we expect the dispersed-phase pressure to be dominated by its kinetic part and therefore $P_{ij} \approx P_{ij}^k = n \langle L_i V_j \rangle \approx (1/2) \rho \phi \langle V_i V_j \rangle$ (cf. Sangani and Didwania [1993a]). We shall non-dimensionalize pressure by $\rho\gamma^2 a^2/2$.

To determine the pressure and velocity variance, we multiply (9) by $\phi V_i V_j$ and integrate over the velocity space to obtain

$$\frac{\partial P_{ij}}{\partial t} + [P_{ji} \delta_{i2} + P_{i1} \delta_{j2} + 2St^{-1} P_{ij}] = \Phi_e(P_{ij}), \quad (11)$$

where, in obtaining the terms inside the square brackets on the left-hand side, use has been of integration by parts, and

$$\Phi_e(P_{ij}) \equiv \phi \int d\mathbf{V} V_i V_j \frac{\partial_e f}{\partial t}. \quad (12)$$

To make further progress we need to determine f and $\Phi_e(P_{ij})$. Exact

solution for f is rather difficult to obtain and hence we have developed approximate methods. First, we develop an approximation in which the shear-induced collisions are neglected in evaluating $\partial_e f/\partial t$, i.e., the actual velocities \mathbf{w} , \mathbf{w}_i , etc. in (10) are replaced by the relative velocities \mathbf{V} , \mathbf{V}_i , etc. The resulting theory will explain the origin of multiple steady states but not the absence of quenched state at high enough Re_s . The theory will be subsequently modified to include the shear-induced collisions which play an important role in the behavior of quenched states.

We have developed two approximate theories for evaluating $\Phi_e(P_{ij})$. Both give identical results. One is based on the method due to Grad [1949] in which f is expanded in a series of Hermite polynomials:

$$f(\mathbf{V}) = \left[1 + \frac{1}{2} \left(a_{ij} - \frac{1}{3} \delta_{ij} a_{kk} \right) \frac{\partial^2}{\partial V_i \partial V_j} + \Lambda \right] f_m, \quad (13)$$

where f_m corresponds to an isotropic Maxwellian distribution. The constant a_{ij} is related to the second moments of velocity and temperature T by

$$\langle v_i v_j \rangle = T(\delta_{ij} + a_{ij}).$$

The trace a_{ii} is zero because the bubble phase temperature is one-third of the velocity variance. The series is truncated keeping only the first two terms and (10) and (12) are evaluated in terms of a_{ij} . Substituting for $\Phi_e(P_{ij})$ in (11) and solving the resulting equations then yields a_{ij} and P_{ij} . In the other method, which we describe in more detail here, we model the collision process as similar to that between Maxwell molecules. Thus, we assume that the force \mathbf{F} between two bubbles is repulsive and along the line joining the center of the two bubbles separated by a distance r with $\mathbf{F} = \kappa r^{-5}$ where κ is a constant of proportionality. For this special case it turns out that the collision term (10) assumes a particularly simple form and one finds

$$\Phi_e(P_{ij}) = \lambda^* \phi (p \delta_{ij} - P_{ij}), \quad (14)$$

where $p = 1/3 P_{kk}$ and λ is a constant related to κ . Now in the limit $St \rightarrow \infty$, we expect the variance to become very large and the collision term on the right-hand side of (9) to dominate leading to an isotropic Maxwellian velocity distribution. The dispersed-phase viscosity will then be expected to approach the viscosity of dilute gas consisting of hard-sphere molecules. Matching with the known expression for that viscosity requires

$$\lambda^* = \lambda T^{1/2} \quad \text{with} \quad \lambda = \frac{24}{5\sqrt{\pi}} \quad (15)$$

$T \equiv \langle V^2 \rangle / 3$ being the bubble phase temperature. This choice of λ^* is equivalent to choosing the force law constant κ of Maxwell molecules to be proportional to T .

Since $T^{1/2}$ in due course will be shown to be $O(1/\phi)$, it should be noted that $\lambda^* \phi = O(1)$ and the right-hand side of (11) is the same order of magnitude as the other terms in that equation in the limit $\phi \rightarrow 0$. Thus, we need to keep the collision term in our analysis even for very dilute suspensions. Now substituting (14) and (15) into (11), using $p = \phi \langle V_i V_j \rangle / 3 = \phi T$, and solving for the steady state conditions, we obtain

$$\frac{P_{11} - P_{22}}{St^{-1} + \phi \lambda T^{1/2}} = \frac{\lambda \phi^2 T^{3/2}}{St^{-1} + \phi \lambda T^{1/2}}, \quad (16)$$

$$P_{12} = -\frac{P_{11}}{2(St^{-1} + \phi\lambda T^{1/2})} = -\frac{\lambda\phi^2 T^{3/2}}{2(St^{-1} + \phi\lambda T^{1/2})^2} \quad (17)$$

and $P_{23}=P_{31}=0$. To complete the solution we need to determine T . This is accomplished by taking the trace of (11) to yield at steady state the energy equation for the dispersed phase

$$P_{12} + 3\phi St^{-1}T = 0 \quad (18)$$

according to which the work done in shearing the suspension is dissipated by the viscous drag. Substituting for P_{12} from (17) into (18) yields a cubic equation for $T^{1/2}$ whose three roots including zero are given by

$$T_1 = 0, T_{2,3} = \frac{5\sqrt{\pi}St}{288\phi} \left[1 - \frac{12}{St^2} \pm \sqrt{1 - \frac{24}{St^2}} \right] \quad (19)$$

where we have used the numerical estimate of λ from (15).

It is easy to show that T_2 corresponds to an unstable state so that the quenched and ignited states we found in numerical simulations (cf. Fig. 1) correspond respectively to T_1 and T_3 . Moreover, we see that the ignited state exists only when $Re_s = 18St$ exceeds a critical value given by $Re_{c*} = 18\sqrt{24} = 88.18\dots$. This explains why the final state is the quenched state regardless of the initial variance for $Re_s = 80$. For $Re_s = 140$, the variance corresponding to the unstable state 2 is approximately 4.3 according to (19). Thus, as discussed in the earlier, if initial variance is smaller than this value, the final state must be the quenched state, and a higher initial variance should lead to the ignited state. Simulations for $Re_s = 140$ qualitatively agree with this prediction although we find that even a slightly higher initial variance of 6 leads to a quenched state. In fact, the variance reaches a maximum of about 15 before eventually decreasing to a vanishingly small value corresponding to the quenched state. This quantitative discrepancy may arise due to a number of reasons including (i) the neglect of shear-induced collisions in the theory, (ii) finite number of bubbles ($N=32$) used in the numerical simulations, (iii) the use of soft core repulsive potential in simulations, and (iv) the neglect of hydrodynamic interactions in the theory. Finally, we see that the theory we have presented fails completely in the case of $Re_s = 170$ in predicting the existence of only one stable state.

The theory we have presented so far is adequate for determining the steady state variance in the ignited state for which the root-mean-squared velocity is much greater than γ_a and for giving the criterion for extinction of the ignited state, i.e. $Re_s < Re_{c*}$. However, the preceding theory gives poor estimates for T_1 and T_2 because it neglects shear-induced collisions which are important for these two states.

To improve the theory, we now consider the limit in which the root-mean-square velocity is much smaller than γ_a , a situation applicable to the quenched state. Since the collisions are infrequent in this state, $\tau_v \ll \tau_c$ and the majority of bubbles travel with the velocity of the fluid. Therefore, in this limit $\Phi_e(P_{ij})$ (cf. (12)) can be determined from simple geometric considerations by using $\mathbf{w} = \langle \mathbf{u} \rangle$ to yield

$$\Phi_e(P_{11}) = 2\Phi_e(P_{22}) = 8\Phi_e(P_{33}) = \frac{512}{315\pi}\phi^2, \quad \Phi_e(P_{12}) = -\frac{8}{35}\phi^2 \quad (20)$$

and $\Phi_e(P_{13}) = \Phi_e(P_{23}) = 0$. Substituting for $\Phi_e(P_{ij})$ from (18) into (9) and solving for steady state conditions yield

$$P_{11} = 4P_{33} = \frac{256}{315\pi}St\phi^2, \quad P_{22} = \frac{64}{315\pi}St^3\phi^2 \left[1 + \frac{4\pi}{St} + \frac{9}{8St^2} \right], \quad (21)$$

$$P_{12} = \frac{64}{315}St^2\phi^2 \left[1 + \frac{9\pi}{16St} \right]. \quad (22)$$

Thus, the quenched state variance is dominated by the value of $\langle V^2 \rangle$ and equals roughly $(64\pi/315)St^2\phi$ in the limit of small ϕ for Stokes numbers of magnitude 5 or greater. At $\phi = 0.005$ and $Re_s = 18St = 140$, the conditions for the simulations shown in Fig. 1, this gives an approximate variance of 1.5 whereas the simulation gave a vanishingly small number. This occurs because the bubbles arrange themselves eventually in positions where avoid collisions making their velocities the same as the local fluid velocity and it is therefore an artifact of the simulation with periodic boundary conditions. It is possible to avoid this problem in simulations that neglect hydrodynamic interactions by using the Direct-simulation Monte Carlo method [Kumaran et al., 1993].

We have shown that the ignited state exists for all $Re_s > Re_{c*}$. Now we shall determine in what part of this regime, one has multiple steady states and in what portion only the ignited state exists. If the shear-induced variance $Re_s^3\phi$ is greater than the variance of the unstable state 2, i.e. $\mathcal{O}(Re_s^3\phi^{-1})$ (cf. (19)), then the imposed shear will create enough velocity fluctuations to take the suspension past the unstable state 2 even when the initial variance is zero. Consequently, only the ignited state will exist when $Re_s^3\phi$ exceeds a certain $\mathcal{O}(1)$ number. To estimate this number we constructed an *ad-hoc* approximation for $\Phi_e(P_{ij})$ by superimposing its values in the two limits as given by (14) and (20). Solving the resulting equations for P_{ij} at steady state yielded a quadratic equation in $T^{1/2}$. One root of this equation is always negative and the other three correspond qualitatively to the three solutions (quenched, unstable, and ignited) given by (19). However, when ϕ is increased from zero at a fixed value of $St = Re_s/18$ that is greater than $\sqrt{24}$, we now find that the quenched and unstable state variances approach each other. The variances of these two states become equal at

$$\phi_c = \left(\frac{7875\pi^2}{2304} \right)^{1/3} St^{-3}, \quad \text{or} \quad St^3\phi_c = 3.231K \quad (23)$$

For $\phi > \phi_c$ the two roots become complex so that the only physically meaningful solution to the equations corresponds to the ignited state.

The above criterion can also be used for estimating Re_s beyond which the only steady state is the ignited state for given ϕ . At $\phi = 0.005$, this yields the transition Re_s of 155.6. This is in agreement with the simulations shown in Fig. 1 for which the multiple states are observed at $Re_s = 140$ but only the ignited state at $Re_s = 170$.

2. Comparison with Simulations

We now compare the theory and simulations in more detail. Fig. 3 is the phase diagram of quenched, ignited, and multiple (quenched plus ignited) states for bubbly liquids. For small ϕ we expect only the quenched state when Re_s is less than 88 and the multiple (quenched plus ignited) states for $Re_s > 88$ and $\phi Re_s^3 > 3.231 \times 18^3 = 18843$. For each value of ϕ , we carry out simulations at different values of Re_s with an initial variance of zero and determine the critical value of Re_s for which the final state is ignited. The pluses are the results obtained by simulations with $N=32$ and full hydrodynamic interactions together with the soft core repulsive potential for overlap-

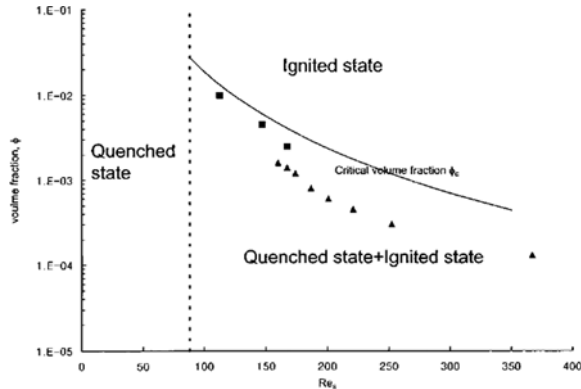


Fig. 3. Multiple steady states-ignited state transition. The solid curve is the theory prediction from kinetic theory and squares and triangles are, respectively, the results of simulations with and without hydrodynamic interactions.

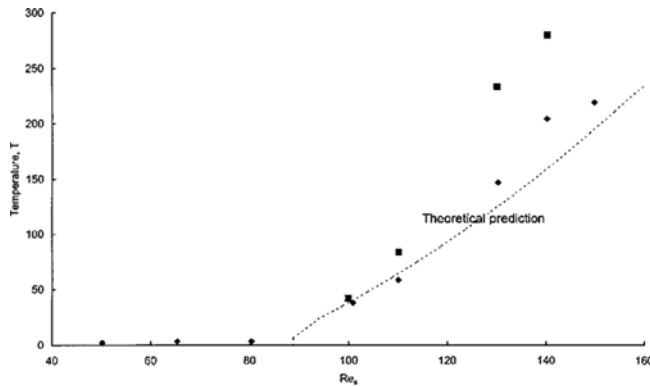


Fig. 4. Temperatures with respect to Reynolds numbers for $\phi=0.03$ with theoretical predictions as shown dashed line. The squares are the results obtained from the simulations with soft-core potential, and diamonds are the results for hard core potential.

ping bubbles as described in section 2. For the purpose of comparison with the theory which neglected the hydrodynamic interactions altogether and modeled the collision process as that corresponding to hard spheres, we also carried out another set of simplified simulations in which these conditions were satisfied exactly. These simulations with $N=100$ are shown by circles. The latter results were also confirmed to be free from finite N effects by another method [Direct-simulation Monte Carlo, Kumaran et al., 1993]. We believe that the better agreement obtained with the full hydrodynamic interaction calculations represented by the pluses is fortuitous.

Fig. 4 shows a comparison between the theory (cf. (19)) and simulations at $\phi=0.03$ varying Reynolds number. For this ϕ , the critical Re_s for multiple steady states to exist is about 86 which approximately coincides with the extinction of the ignited state branch so that we observe only the ignited state at larger Re_s . The simulation results indicated by filled circles were obtained with full hydrodynamic interactions and soft core potential. We find that there is considerable discrepancy between the theory and simulations. This results from the use of soft core potential in simulations which allow bubbles to overlap considerably resulting in a decrease in the apparent volume fraction of bubbles. Since the variance varies roughly

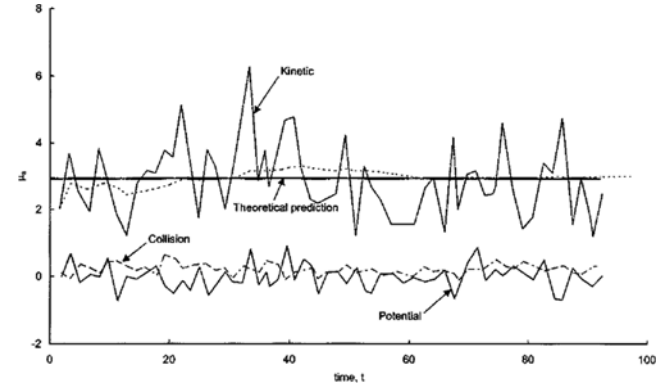


Fig. 5. The kinetic, collisional, and hydrodynamic contributions to the bubble-phase shear viscosity for $Re_s=150$ and $\phi=0.03$.

as $1/\phi^2$, the use of soft core potential results in a higher variance. To correct for this effect we carried out simulations with no hydrodynamic interactions with both soft as well as hard core potentials. The open circles in Fig. 4 represent the results obtained by multiplying the results of full hydrodynamic interactions with the correction ratio accounting for the use of soft core potential. We see that with this correction, the theory and simulations are in very good agreement with each other.

Fig. 5 shows the kinetic, collisional, and hydrodynamic (or potential) contributions [cf. Sangani and Didwania 1993a; Bulthuis et al., 1994 for definitions] to the dispersed-phase shear viscosity (non-dimensionalized by $1/2\rho\gamma^2$) $\mu_s = -P_{12}$ as time progresses. As expected, the collision and potential parts are seen to make negligible contributions to the overall value of shear viscosity at $\phi=0.03$. Note that potential interaction between bubbles is still significant in dynamics. The average value of the kinetic part is seen to be in a very good agreement with the value predicted by theory (cf. (17)) provided that we use the value of average variance computed in simulations to substitute for T instead of using (19). This distinction is necessary to make since T for the soft core potential is different from the theoretical estimate.

Fig. 6 shows a comparison between the theory and simulations for P_{22}/P_{11} . The computed values include the collision and hydrodynamic parts also. Once again we see a reasonable agreement between the two. More importantly, it must be noted that the dispersed-phase exhibits considerable normal stress differences.

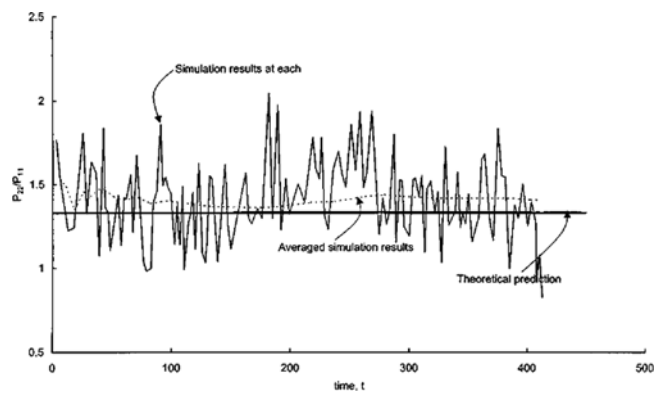


Fig. 6. P_{22}/P_{11} as a function of time for $Re_s=150$ and $\phi=0.03$.

Finally, we note that a discrepancy that still remains between the theory and simulations is the rather high value of the maximum variance seen in Fig. 1 for the quenched state simulation with $Re_s=140$. Even after accounting for the shear-induced variance, our approximate theory estimates the variance of the unstable state 2 to be approximately 5 which is much lower than the maximum value of about 15 obtained in the simulation. Thus, it appears that our theory underestimates the magnitude of the variance in the unstable state.

CONCLUDING REMARKS

In this paper we have addressed the problem of the dispersed-phase rheology in suspensions of spherical bubbles at relatively large Reynolds numbers. We found that the rheology is quite complex even when the microscale physics governing the bubble motion is considerably simplified in terms of lift and viscous forces. The key to understanding the results of simulations has been to appreciate the dependence of the dispersed-phase viscosity on its temperature. This dependence is nonlinear and gives rise to multiple steady states. The calculations presented here also show a need to include the energy balance and temperature in the averaged description of flows of suspensions.

Our simulations and theory have thus far been restricted to small ϕ where the shear-induced fluctuations are the largest. We have extended the theory to higher volume fractions by using the theory of dense gases and Grad's moment expansion approximation (cf. (13)). The predictions of this theory are being currently tested for non-dilute suspensions.

One motivation of this study was to investigate the possibility that the presence of shear may stabilize bubbly liquids. We can now make a rough estimate of when stabilization is possible. At present we are studying the flow of bubbly suspension under simple shear in the presence of gravity.

In that case the dispersed-phase pressure depends on both the mean relative velocity of the bubbles induced by buoyancy and lift forces and mean shear rate. The mean relative motion gives a negative contribution to the pressure via hydrodynamic contribution as shown in Sangani and Didwania [1993a], while the shear gives a positive contribution via the kinetic and collision contributions. An exact criterion for the stability has not been determined yet, but preliminary calculations (simulations) already show that the suspension is stable at least when the Reynolds number based on shear is in the ignited state regime. Thus, let us take $Re_p = \rho \gamma a^2 / \mu = 100$ for the purpose of estimating when shear may play an important stabilizing role. For 1 mm radius bubbles in water, this requires $\gamma \approx 100 \text{ s}^{-1}$. For air-water system with $\gamma a = 10 \text{ cm/s}$, the small We approximation is justified since $We \approx 0.14$. To provide γ of 100 s^{-1} in a flow of bubbly suspension through a pipe of radius R (in cm) we need the mean flow rate to be $100R$ (in cm/s). Since we are dealing with large Reynolds numbers, one question that immediately comes to mind is what if the turbulence would set up much before the high shear required for the ignited state. Taking the mean flow rate to equal γR , the Reynolds number Re_p based on the pipe radius will be $100(R/a)^2$. This will be indeed quite large for many practical applications. However, it should also be noted that the turbulence will be considerably delayed due to high Reynolds stress created by the velocity fluctuations induced by the presence of shear. A parameter

that is expected to be more important in determining the onset of turbulence is $Re_p^* = Re_p \mu / \mu^*$, the Reynolds number based on the effective viscosity μ^* of the mixture. From the definition of the mixture stress given in Biesheuvel and Wijngaarden [1984] and Sangani and Didwania [1993a], we find that the effective viscosity of the mixture in the ignited state is close to the dispersed-phase viscosity, or, in the present example, $\mu^* \approx 100 \mu$. Thus, in fact, it is possible to have a significant range of R/a and Re_p values over which the mean flow will be steady and one-dimensional. We hope to carry out a more detailed analysis based on averaged equations to test this speculation in our future work.

ACKNOWLEDGMENT

S.-Y. Kang acknowledges the support for this work by the BK21 Program.

REFERENCES

- Auton, T. R., Hunt, J. C. R. and Prud'homme, M., "The Forces Exerted on a Body in Inviscid Unsteady Non-Uniform Rotational Flow," *J. Fluid Mech.*, **197**, 241 (1988).
- Bando, Y., Kuze, T., Sugimoto, T., Yasuda, K. and Nakamura, M., "Development of Bubble Column for Foam Separation," *Korean J. Chem. Eng.*, **17**, 597 (2000).
- Biesheuvel, A., "Structure and Stability of Void Waves in Bubbly Flows," in *Waves in Liquid/Gas and Liquid/Vapor Two-Phase Systems* (ed. S. Morioka and L. van Wijngaarden), Proc. IUTAM Sympos., Tokyo, Japan, 1, 1994 (Kluwer Academic, 1995).
- Biesheuvel, A. and Gorissen, W. C., "Void Fraction Disturbances in a Uniform Bubbly Fluid," *Int. J. Multiphase Flow*, **16**, 211 (1990).
- Biesheuvel, A. and van Wijngaarden, L., "Two-Phase Flow Equations for Dilute Dispersion of Gas Bubbles in Liquid," *J. Fluid Mech.*, **148**, 301 (1984).
- Bulthuis, H. F., Prosperetti, A. and Sangani, A. S., "Particle Stress" in *Disperse Two-Phase Potential Flow*, *J. Fluid Mech.*, **294**, 1 (1995).
- Chapman, S. and Cowling, T. G., "The Mathematical Theory of Non-Uniform Gases," 3rd Edn., Cambridge University Press (1970).
- Grad, H., "On the Kinetic Theory of Rarefied Gas," *Commun. Pure Appl. Math.*, **2**, 331 (1949).
- Hasimoto, H., "On the Periodic Fundamental Solutions of the Stokes Equations and their Application to Viscous Flow Past a Cubic Array of Spheres," *J. Fluid Mech.*, **5**, 317 (1959).
- Kim, S. J., Cho, Y. J., Lee, C. G., Kang, Y. and Kim, S. D., "Diagnosis of Bubble Distribution in a Three-Phase Bubble Column Reactor for Dehydration of Ortho-Boric Acid," *Korean J. Chem. Eng.*, **19**, 175 (2002).
- Kumaran, V., Tao, H.-K. and Koch, D. L., "Velocity Distribution Function for a Bidisperse, Sedimenting Particle-Gas Suspension," *Int. J. Multiphase Flow*, **19**, 665 (1993).
- Ladd, A. J. C., "Hydrodynamic Transport Coefficient of Random Dispersions of Hard Spheres," *J. Chem. Phys.*, **93**, 3484 (1990).
- Lessard, R. R. and Zieminski, S. A., "Bubble Coalescence and Gas Transfer in Aqueous Electrolytic Solutions," *Ind. Eng. Chem. Fundam.*, **10**, 260 (1971).
- Sangani, A. S. and Didwania, A. K., "Dispersed-Phase Stress Tensor in Flows of Bubbly Liquids at Large Reynolds Number," *J. Fluid Mech.*,

248, 27 (1993a).
Sangani, A. S. and Didwania, A. K., "Dynamic Simulations of Flows of Bubbly Liquids at Large Reynolds Numbers," *J. Fluid Mech.*, **250**, 307 (1993b).
Sangani, A. S., Zhang, D. Z. and Prosperetti, A., "The Added Mass, Basset, and Viscous Drag Coefficients in Nondilute Bubbly Liquids Undergoing Small-Amplitude Oscillatory Motion," *Phys. Fluids A*, **3**, 2955 (1991).
Smereka, P., "On the Motion of Bubbles in a Periodic Box," *J. Fluid Mech.*, **254**, 79 (1993).
Tsao, H.-L. and Koch, D. L., "Collisions of Slightly Deformable, High Reynolds Number Bubbles with Short-Range Repulsive Forces," *Phys. Fluids*, **6**, 2591 (1994).
Zhang, D. Z. and Prosperetti, A., "Averaged Equations for Inviscid Disperse 2-Phase Flow," *J. Fluid Mech.*, **267**, 185 (1994).